

# Leppe (Germany)

## Geophysical survey summary

MAY 2020



---

**SUBJECT:** ...

report     
  information     
  consideration     
  decision

**To:** ...     
 **From:** University of Liège & British Geological Survey

---

**Index**

Leppe.....	3
Summary of the study area .....	3
Summary of available ground truth data .....	3
Geophysical investigations.....	4
Correlation analysis .....	14
Resource Distribution Model .....	16
Conclusion.....	20
References.....	21
Contact.....	22

## Leppe

### Summary of the study area

#### Site history

The Leppe landfill is a municipal solid waste (MSW) landfill that is operational since 1982 as the disposal centre of Leppe (:metabolon) located in Lindlar, Nordrhein-Westfalen, Germany. Until the end of 2004, MSW was deposited in five disposal areas DA1, DA2, DA3, DA4 and DA5 (see *Figure*). Since 2005, only ash from municipal solid waste incineration are deposited in DA4 and DA5 on top of the municipal solid waste and in mono-deposition in DA6. A landfill capping in DA1-5 enables the extraction of biogas to a rate of about 450 – 500 m<sup>3</sup>/h.

#### Summary of available ground truth data

To improve gas extraction, nine gas wells were drilled during the first drilling campaign in 2017 in the areas DA3 and DA5. From each drilling, several samples at different depths were taken to analyse the remaining gas production potential. In addition, 11 boreholes were drilled during the second sampling survey in 2018 mostly in the areas DA3 and DA4. For each borehole a log description is available. The topography prior to landfill activities is available so that with recent digital elevation model it is possible to know the volume of each disposal zones.

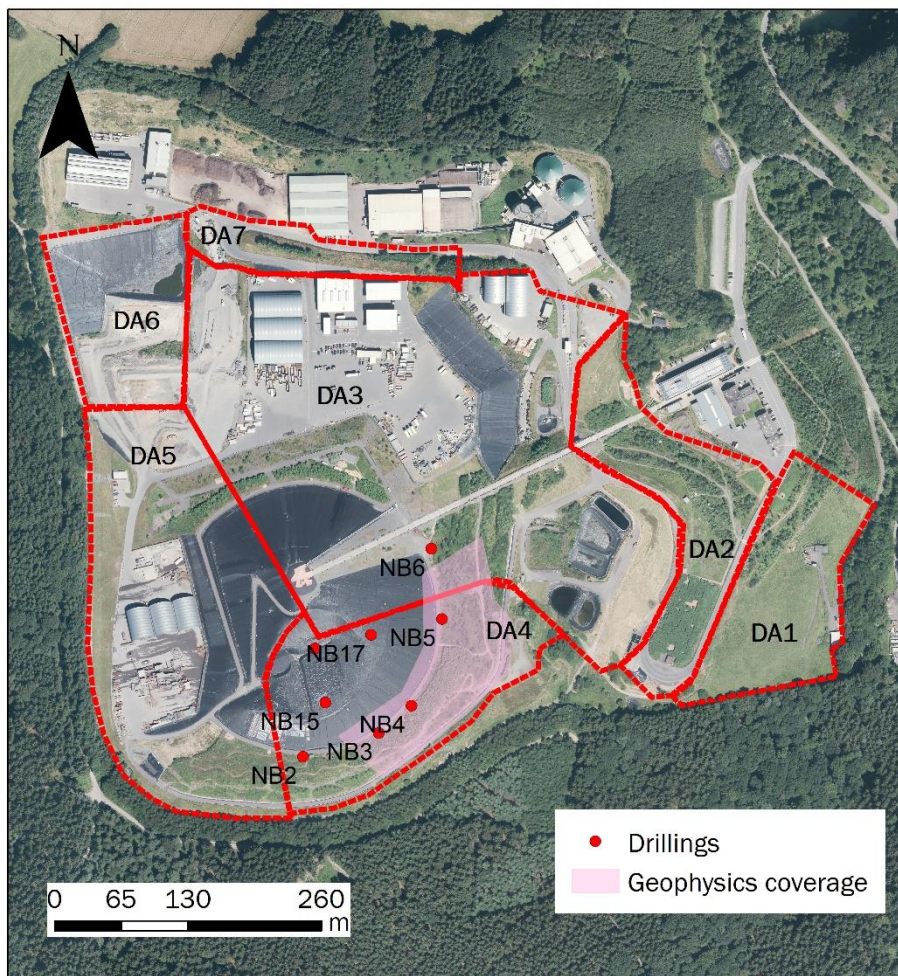


Figure 1: Overview of the Leppe landfill. Red dashed lines represent the different disposal areas of the site (DA1-DA7) and red dots are the boreholes close the geophysical surveyed zone shown in pink.

## Geophysical investigations

### Geophysical methods and coverage

The geophysical survey was carried out from 21<sup>st</sup> to 23<sup>rd</sup> of October 2019.

Due to logistics and the infrastructure constraints (*i.e.* complete cone built from waste incineration ash, presence of a geomembrane), the geophysical survey was focused in zone DA4 (*Figure 1*) underneath the cone (see *Figure* ). Only the boreholes located within the zone were used for further calibration (NB2-NB6, NB15, NB17 in *Figure 1*). In addition, we expected that the site infrastructure would cause large conductivity values at shallow depths as well as overall large values of magnetic susceptibility. Therefore, we did not use mapping methods (limited depth of exploration). Instead, we applied profiling methods including 3D Electrical Resistivity Tomography (ERT) and Induced Polarization (IP), Multichannel Analysis of Surface Waves (MASW) and Horizontal to Vertical Noise Spectral Ratio (H/V) to obtain detailed information about changes of geophysical properties with depth (see implementation in *Figure 1*).

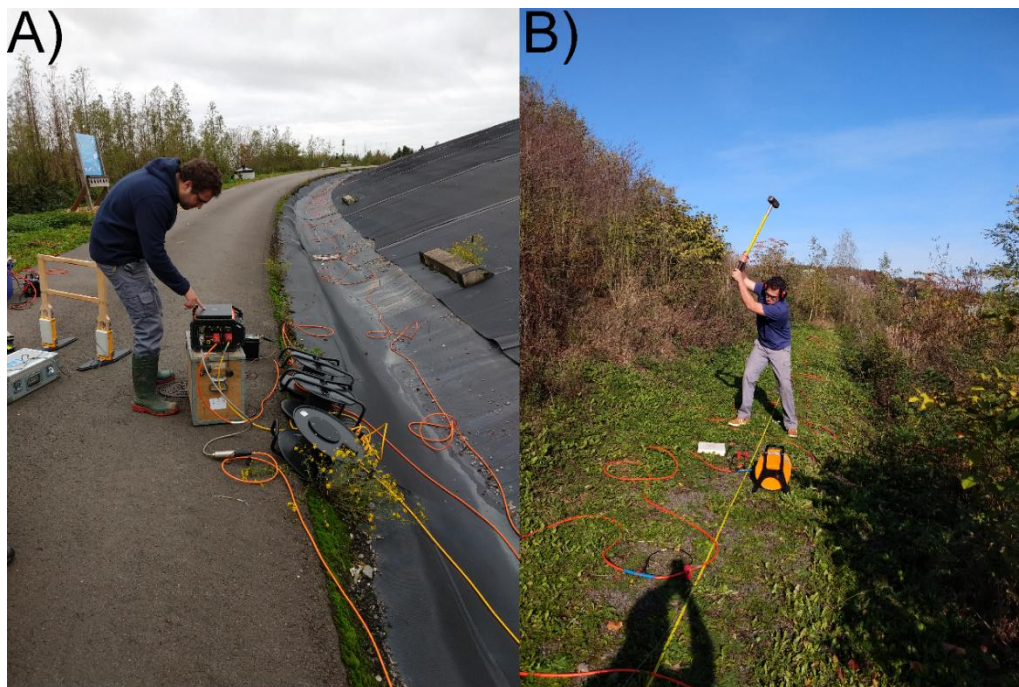


Figure 1: A) ERT and IP acquisition, B) MASW set-up.

In the following, the measurement parameters and spatial coverage of each method are summarized in more detail.

ERT and IP data were acquired with an ABEM Terrameter LS system. To derive a 3D resistivity/IP model, two nearly parallel profiles were deployed mostly in zone DA4, at the bottom part of the landfill cone and along the road southwards (*Figure 2*). Each profile contained 64 stainless steel electrodes, which were planted through the liner. The electrode spacing was 3 m and the spacing between the profiles was approximately 55 m. For the data acquisition, we used a combination of a dipole-dipole array with a 'n' factor equals to 6, a gradient array with a 's' factor equals to 8 (Dahlin and Zhou, 2006) and a bipole-bipole array. Measurements were not only carried out inline but also crossline. Electrical current injection was setup to 2 s (delay of 0.8 s and acquisition of 1.2 s) and voltage decay was measured

during 1.86 s after current shut down. Measurements were repeated twice to estimate the repetition error. A sample of reciprocal measurements was also collected for each profile to assess the quality of data.

A *MASW* profile was deployed in the area between the geoelectric profiles mentioned above, but it had to be shifted towards zone DA3 to find a smooth topography and a layer of soil allowing a better coupling (*Figure 2*). The data was acquired using a DAQlink 4 system and a fixed receiver array of 48 vertical geophones (4.5 Hz natural frequency) at 2 m intervals. A 5 kg sledgehammer was used as a source together with a ground-coupled nylon plate. The receiver array was kept fixed and the source was moved every two geophones (4 m) from off one extreme of the spread. In order to increase the signal to noise ratio, a total of 20 shots were stacked at each shot point.

For the *HVSRN* acquisition, we used the seismometer LE-3Dlite MkIII (Lennartz) which is a 3-component sensor that has a low cut-off frequency of 1 Hz. We recorded the ambient noise at 17 locations along the upper ERT/IP profile in the zone DA4 (*Figure 2*). The HVSRN stations were deployed with a spacing of 12 m and the recording time at each point was set to 20 minutes.

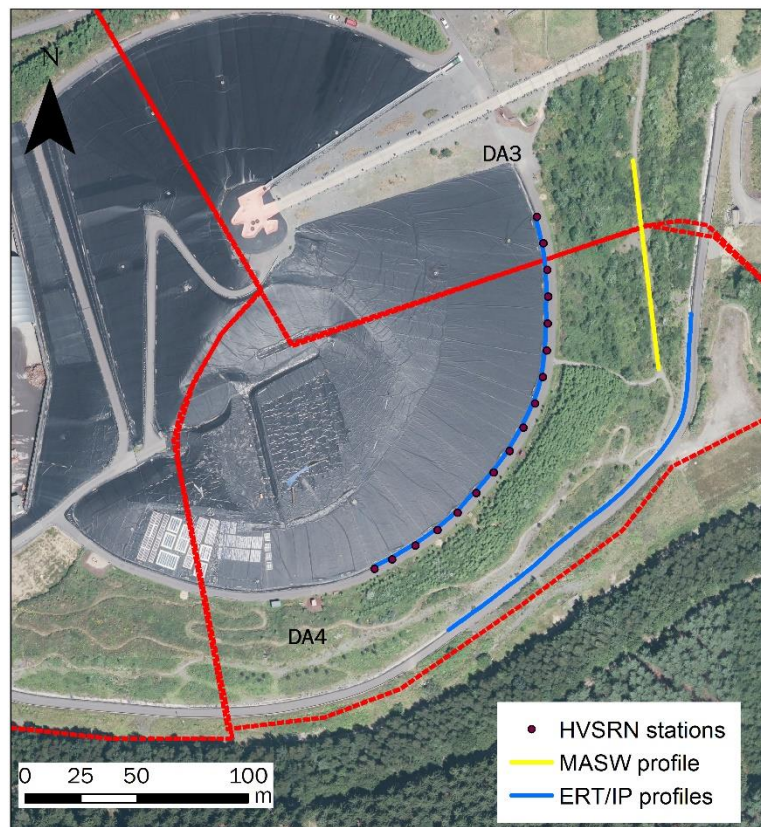


*Figure 2: Geophysical survey including ERT/IP profiles (blue lines), the MASW profile (yellow line) and HVSRN recording stations represented with purple dots.*

## Geophysical processing and results

### ERT and IP results

Data collected were first filtered by removing all measurements characterized by a repetition error on the measured resistance larger than 5%. Then in order to weight the data in the inversion process, individual data errors were calculated using the reciprocal data collected during the acquisition. The weighted data were inverted with BERT (Günther *et al.*, 2006) using a robust constraint on the data and a blocky constraint on the model. The 3D model obtained with BERT satisfies the error weighted chi-square,  $\chi^2 = 1$  meaning that the data are fitted to their error level. *Figure 3* shows the final 3D resistivity and chargeability models. *Figure 4* displays five slices cut through the 3D models. *Figure 5* and *Figure 6* illustrate cross-sections passing close to borehole data (see their location in Fig. 1) allowing appraising the model quality. Note that all coordinates are expressed in European Terrestrial Reference System 1989 – TM32.

3D resistivity and chargeability models (*Figure 3*) display contrasted electrical signatures. First, they seem to contain surface artefacts (especially the chargeability model – *Figure 3B*) close to the electrode positions. This is a common issue that does not much affect the results at depth. In general, the electrical resistivity observed is very low (98.9% of resistivity modelled is below 100 Ohm.m) with the western part of the model exhibiting the lowest values (<10 Ohm.m). This is clearer when looking at slices cut in the 3D model (*Figure 4A*). However, the latter area is also the one with the lowest sensitivity (*Figure 4C*) and should be interpreted with caution. The chargeability model shows greater variability with depth, with a clear transition from low to high chargeability values at depths between 10 and 20 m (*Figure 4B*). *Figure 5* and *Figure 6* allow further interpretation of the models obtained by providing a direct comparison with borehole data. As already introduced above, the resistivity model rather exhibits a lateral contrast. The low resistivity in the western zone of the model can be related, in general, to a higher content of ash and household waste (but it is not possible to differentiate one material from the other due to low model sensitivity in the area). Higher resistivity is due to a higher content of inert materials and the geological host rock. However, the vertical resistivity contrast is not strong and does not allow the base of the landfill to be inferred. The vertical variations observed in the chargeability sections are more pronounced. In general, the inert materials are characterized by low chargeability (<20 mV/V), the household waste by medium chargeability (between 20 and 60 mV/V) and the geological host rock by high chargeability (>60 mV/V). The base of the landfill can be therefore deduced from chargeability sections. Nevertheless, in zones of low sensitivity, the contrast is attenuated and does not allow to image the interface accurately (see *e.g. Figure 5* at X= 389 267 m).

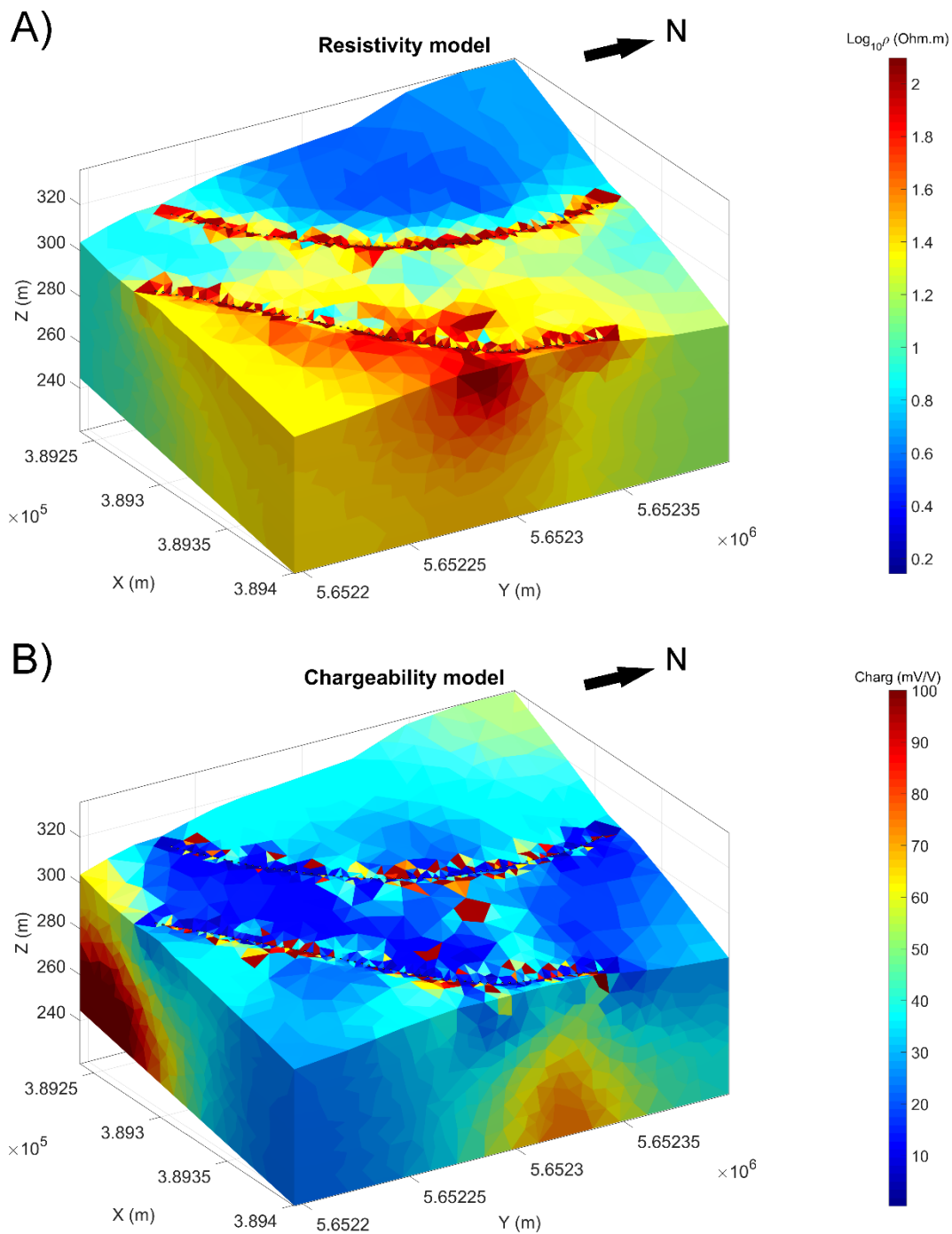


Figure 3: 3D resistivity (A) and chargeability (B) models.

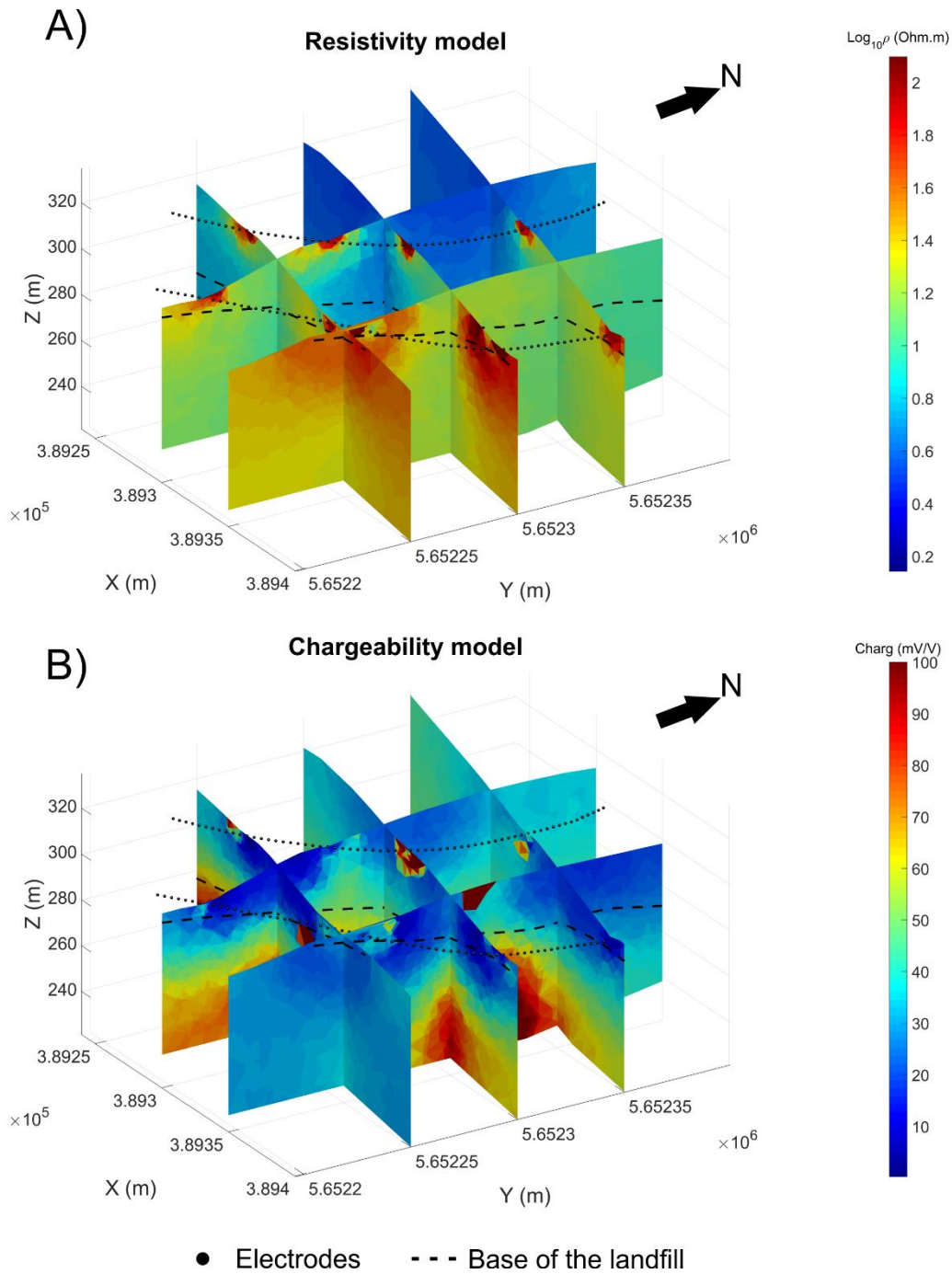


Figure 4: Slices cut through the 3D models at  $X = 389\,250\text{ m}$ ,  $X = 389\,350\text{ m}$ ,  $Y = 5\,652\,250\text{ m}$ ,  $Y = 5\,652\,300\text{ m}$  and  $Y = 5\,652\,350\text{ m}$ , respectively.

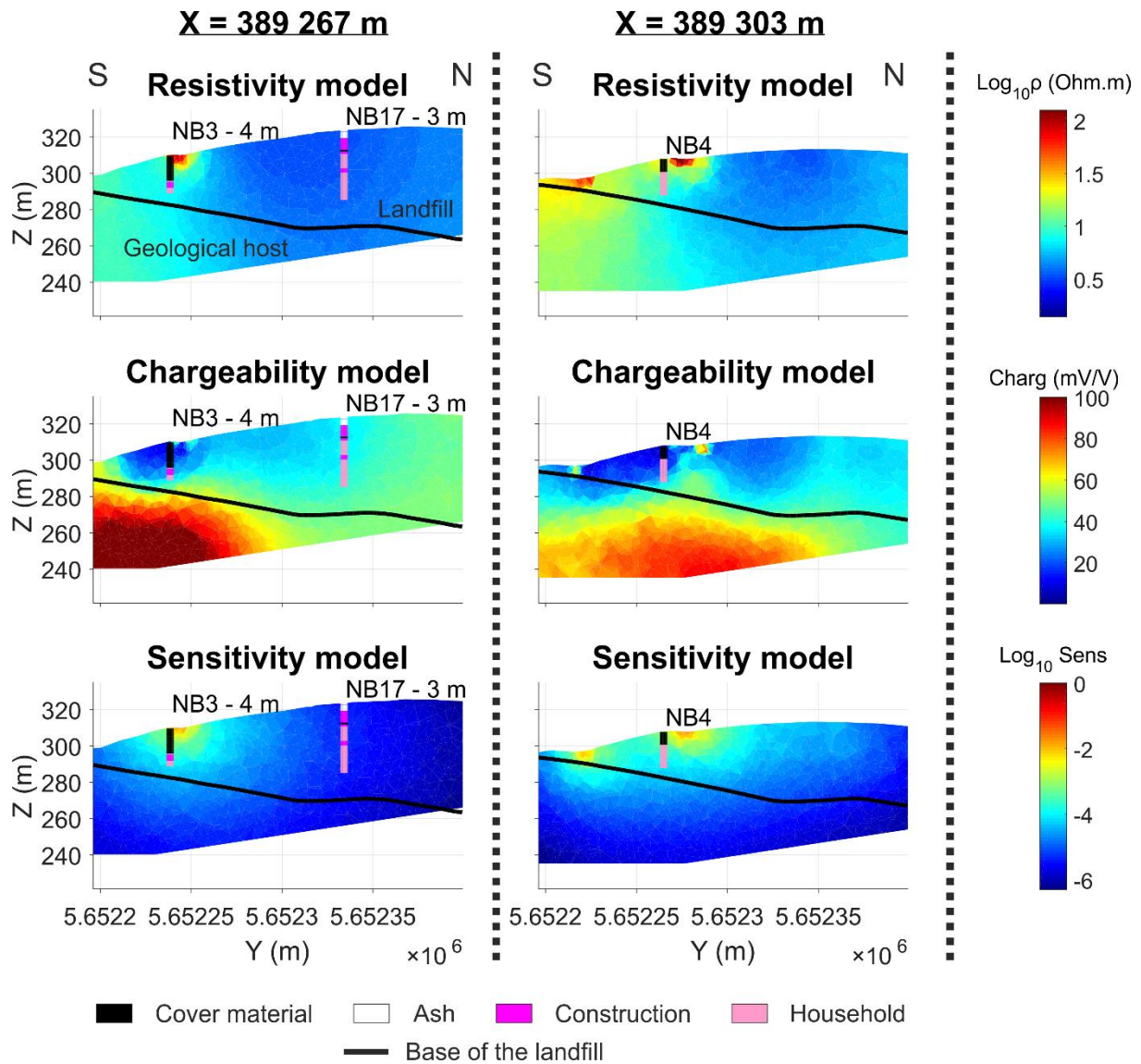
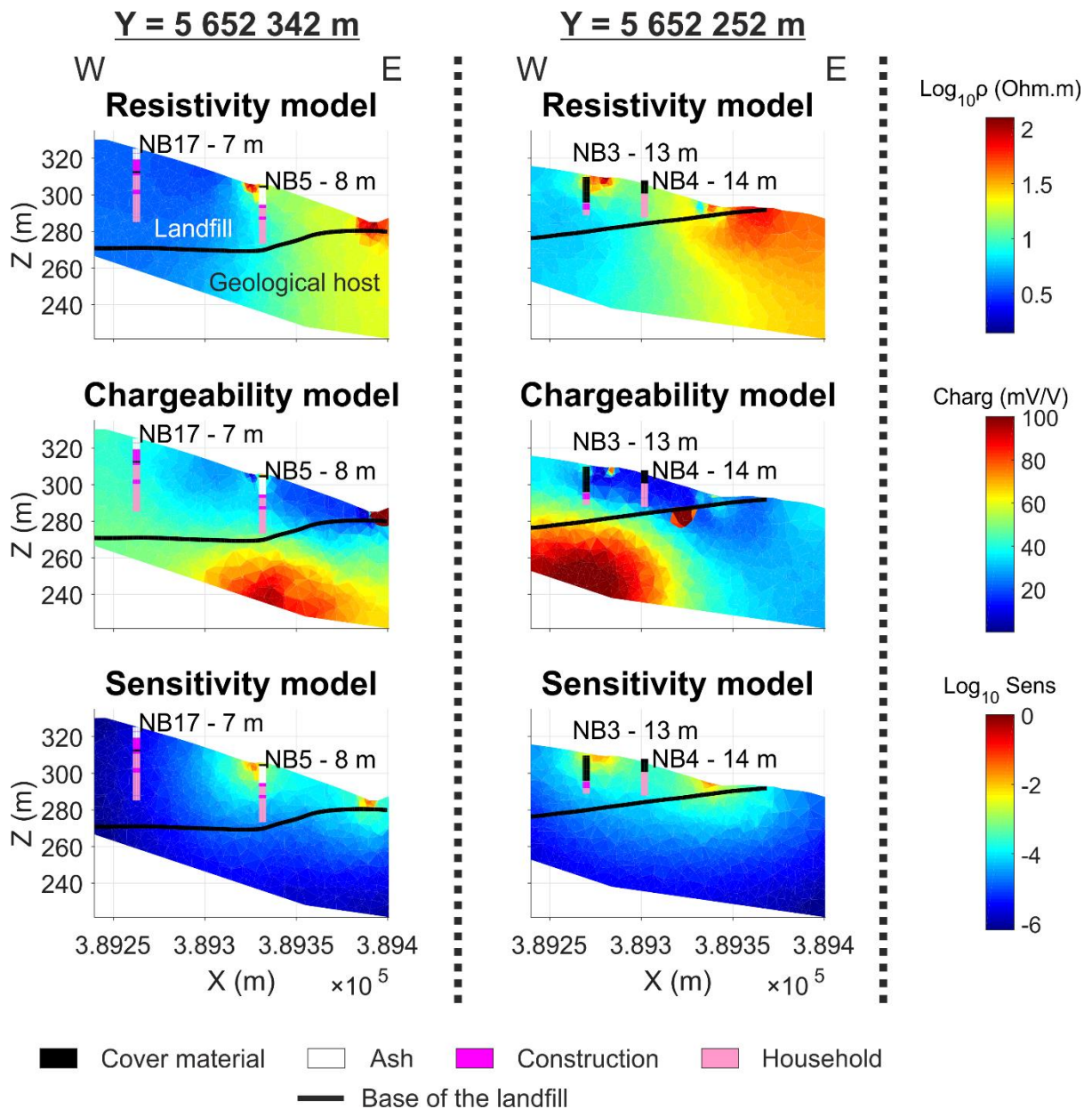


Figure 5: South-north oriented slices of resistivity, chargeability and sensitivity together with borehole logs. The distance indicated next to borehole name represents the distance between the borehole and the profile.



*Figure 6: West-east oriented slices of resistivity, chargeability and sensitivity together with borehole logs. The distance indicated next to borehole name represents the distance between the borehole and the profile.*

### MASW results

We use the software SurfSeis6 (Kansas Geological Survey KGS) to process the data. As we used a fixed spread receiver array, we first emulated a roll-along data acquisition pattern (i.e. twelve 24-channel records). Each shot record was transformed to calculate the phase velocity-frequency distribution, also known as the dispersion curve and the fundamental mode of each dispersion curve was then picked. Finally, we invert the dispersion curves to derive a 2D shear-wave velocity model (see [Figure 7](#)).

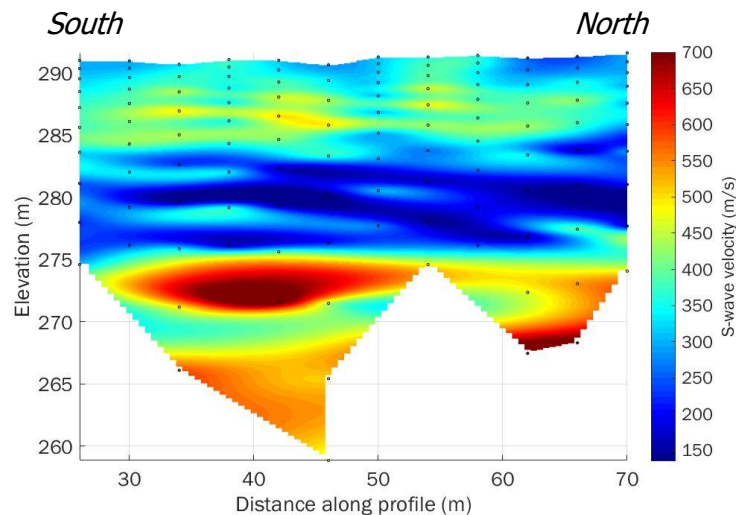


Figure 7: *Shear-wave velocity model from MASW method. Dots represent the locations of the dispersion curves; one column of dots constitutes one dispersion curve.*

The velocity model shows three main heterogeneous layers. The shallowest layer is characterized by intermediate velocities between 400 and 500 m/s. Underneath it, a thicker layer of low velocities from 150 m/s up to approximately 350 m/s is observed. In the bottom part (elevation 275 m), we can see an increase in the velocities up to 700 m/s, that might represent the deepest heterogeneous layer. Although there are no boreholes drilled in the location of the MASW profile, we can make a rough comparison with the borehole NB5 (drilled 40 m west of the profile) where a layer of ash lies on the top of a layer of household waste. This might correspond with the intermediate and low velocity layers observed in the model. Furthermore, the largest Shear-wave velocities might represent the natural soil beneath the waste deposits, which is according to old topographic maps expected to be at a mean elevation of 275 m above sea level along the profile.

### HVSRN results

For the HVSRN processing, we used the open source software GEOPSY (SESAME European Project). At each HVSRN station, we recorded the ambient vibrations in three components: a signal in the north-south direction, east-west and vertical directions. Then, for each station the following process was done: selection of N stationary windows in the three components, computation of Fourier spectra for each window, average of horizontal components, computation of the spectral ratio HVSRN, computation of the average HVSRN ratio ([Figure 9](#)). The time series were slid in windows from 25 s to 40 s (depending on the level of non-stationary noise) and a 70% of overlap, giving between 34 and 82 windows in total.

In the computed HVSRR spectra, one or two fundamental peak(s) - peaks with maximum HVSRR amplitude- were observed (see for instance in *Figure 9*). The values of frequencies associated with one or more spectral peaks are strongly dependent on one or more layers velocities and thicknesses (Piña-Flores et al. 2016). This means that two well separated and defined fundamental peaks in the HVSRR spectrum might be associated with two layers over a half-space.

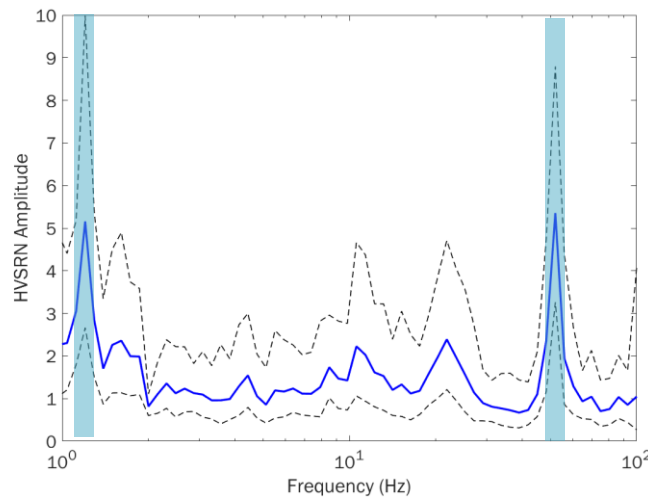


*Figure 9: Computation of HVSRR amplitude at one station. The solid line is the HVSRR amplitude averaged over all the windows and the two dashed lines represent the standard deviation. Note that there are two peaks of high amplitude at 1.2 Hz and 52 Hz.*

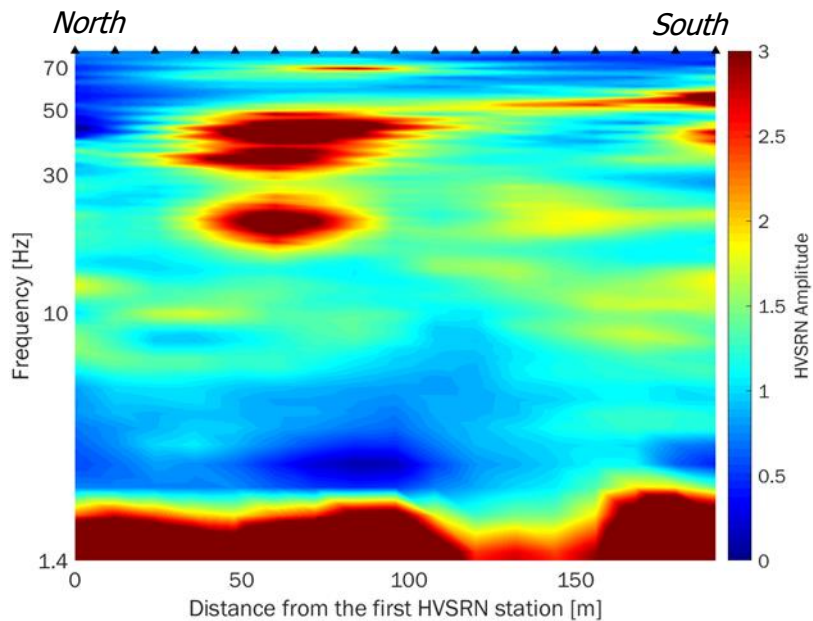


*Figure 8: Interpolation of the HVSRR spectra for all the stations. Triangles in black represent the position of each HVSRR station.*

To visualize the fundamental peak(s) and their continuity along all the stations, we interpolate the HVSRL amplitude along the position of all the stations (see *Figure 8* **Erreur ! Source du renvoi introuvable.**). Here, we can see that there is one fundamental peak centred at around 1.5 Hz for almost all the HVSRL stations. Other contributions can also be observed at high frequencies around 20-50 Hz between the 4<sup>th</sup> and the 8<sup>th</sup> station and again in the last stations (towards the south). In general, the fundamental peaks at low frequencies are associated with layers at larger depths compared to those fundamental peaks at higher frequencies (shallower layers).

Afterwards we transformed the previous results into thicknesses by using a parametric analysis. We used the frequencies linked to two fundamental peaks -  $f_{\beta_1}$  and  $f_{\beta_2}$  - to roughly determine the thickness  $h_1$  and  $h_2$  along all the HVSRL stations. For this purpose, we used the shear-wave velocities estimated before and the formulas:

$$f_{\beta_1} = \frac{\beta_1}{4h_1} \qquad f_{\beta_2} = \frac{1}{4\left(\frac{h_1}{\beta_1} + \frac{h_2}{\beta_2}\right)}$$

where  $\beta_1$  and  $\beta_2$  are the Shear-wave velocities of layers 1 and 2 and  $f_{\beta_1} > f_{\beta_2}$ . If we assume the same tendency of velocities observed from MASW, then  $\beta_1 = 450$  m/s (ash) and  $\beta_2 = 120$  m/s (household). It is important to mention that we selected the two fundamental peaks with the largest HVSRL amplitude, although for most of the stations only one peak was clearly observed. *Figure 10* shows the position of the HVSRL stations with the real height, the original topography before the landfill started, and the estimated thicknesses of the two layers. Notice that the shallowest layer is only present for the intermediate and last stations as the associated fundamental peak was not continuous. By contrast, it was possible to map the bottom limit of the deepest layer, which roughly follows the tendency of topography. This bottom limit estimated with the HVSRL method is in particularly good agreement with the site elevation before the disposal of the household waste.

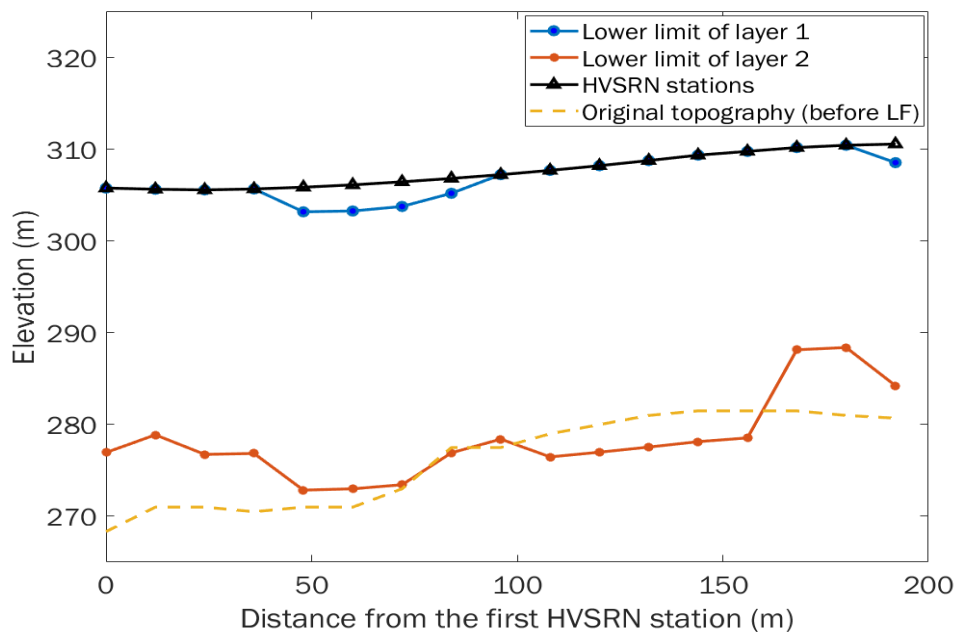


*Figure 10: Location of the HVSRL stations with real topography (solid triangles); the blue dots represent the bottom limit of the first layer and the red diamonds show the lower limit of the deepest layer estimated*

*with the parametric analysis of HVSRN.*

### **Summary of geophysical findings**

Though challenging due to the topography and the infrastructure (presence of a geomembrane, thickness of deposits), the ERT/IP survey allowed to delineate the transition from inert waste to household/ash deposits, but the resolution/sensitivity was not sufficient to individually identify and locate these materials with certainty.

MASW allowed to detect three layers interpreted as: ash (top), household waste (intermediate) and natural soil (bottom). Unfortunately, no ground truth data was available in the vicinity of the profile to validate the provided interpretation. The HVSRN results after the parametric analysis proved to be useful to map the bottom of the landfill.

### **Correlation analysis**

The aim of the correlation analysis is to compare the measured geophysical properties to the different material types found in the landfill. This analysis has two purposes, first to evaluate the effectiveness of each geophysical method in distinguishing different material types and second to choose the relevant geophysical properties to build the Resource Distribution Model at a later step.

The first step for the correlation analysis consists in extracting the geophysical parameters of interest at the location of the boreholes (i.e. NB3, NB4, NB5 and NB17). Three main categories of waste were considered: inert materials (including cover materials and construction waste), household waste and ash. Selected geophysical parameters are the electrical resistivity and chargeability. Parameters provided by the seismic methods were not retained because they mainly deliver information on the location of the bottom of the landfill, which is in fact already known (see *Figure 12*). In addition, the MASW profile is located away from any boreholes that could be used for validation. After parameters extraction, correlations between them are analysed. Note that for legibility reasons, only 50 points from the natural ground were randomly selected for the correlation analysis. The plots shown indicate different sensitivities of selected geophysical parameters. Chargeability tends to increase with depth and decrease with increasing resistivity. From the probability density functions, chargeability seems the most promising to discriminate the different materials present in the landfill (see peaks in *Figure 11*).

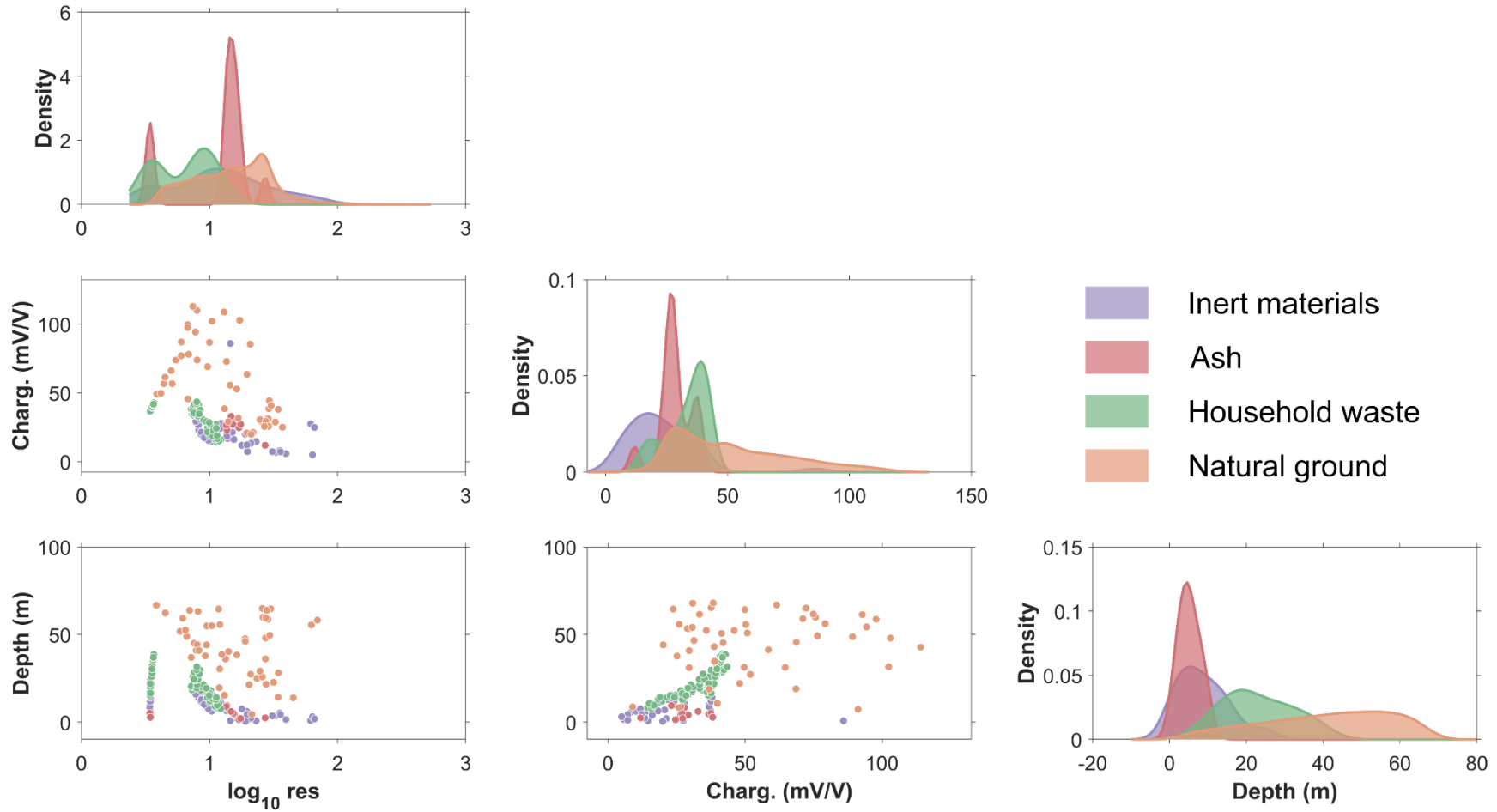


Figure 11: Correlation analysis and probability density functions.

## Resource Distribution Model

From the information collected, we build a Resource Distribution Model (RDM) of the site in different stages. First, we determine the total volume of anthropogenic deposits using the site's Digital Elevation Model (DEM) and historical topographic maps. Next, we focus on the study area and analyse correlations between sampling and geophysical data. Finally, we use supervised machine learning with a neural network algorithm for pattern recognition to build the resource distribution model of the surveyed area.

### Volume of the whole landfill

First, we use the latest available DEM of the site and old topographical maps (before landfill operations) to estimate the total volume of the anthropogenic deposits. As can be seen in *Figure 12*, the landfill was built in a U-shaped valley. Considering both the current DEM and the old topography, the estimated total volume is approximately 8,500,000 m<sup>3</sup>.

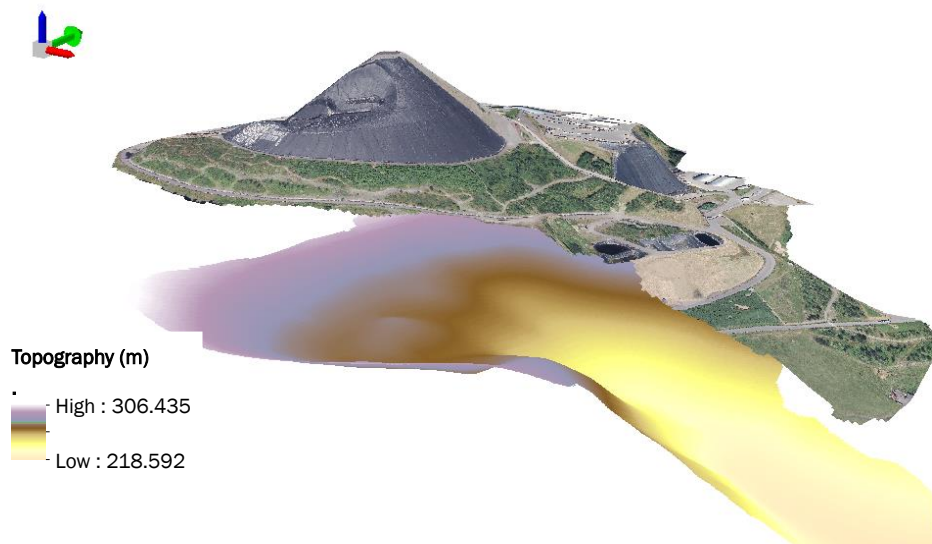


*Figure 12: DEM of the current site with an aerial view on the top and (below) original topography prior to the landfilling of the waste. DEM data and other images are taken from the Nordrhein-Westfalen Geoportal (<https://www.geoportal.nrw/>).*

### Detailed RDM

The RDM proposed here below is limited to the part of the landfill which was actually investigated by geophysics (see *Figure 13*). The area covered is 32,700 m<sup>2</sup>. To build the RDM, the geophysical parameters of interest are extracted at the location of the boreholes (i.e. NB3, NB4, NB5 and NB17) in a similar manner to the correlation analysis. Then a neural network is trained with the selected data (i.e. electrical resistivity, chargeability and position). Since the depth of the natural ground is known throughout the surveyed area, it was decided not to include related parameters in the training and pattern recognition step. The network built is composed of 30 hidden layers. The confusion matrix shown in *Figure 38* offers a way to measure the performance of the machine learning classification. Classes 1, 2 and 3 correspond respectively to inert materials, ash and household waste. The column on the far right of the plot shows the percentage of all examples predicted to belong to each class that are correctly (and incorrectly) classified whereas the row at the bottom of the plot shows the percentage of all the examples belonging to each class that are correctly (and incorrectly) classified. The overall accuracy is shown in the bottom right corner. Given the limited data available, the overall accuracy (almost 92%) is good. Once the network trained, all the parameters of the 3D ERT/IP models located

above the natural ground are fed to the network, which predicts their belonging to one of the three classes. The result of the classification is shown in *Figure 39* for the surveyed area. The estimated volume of each class of material is shown in *Table 1*.

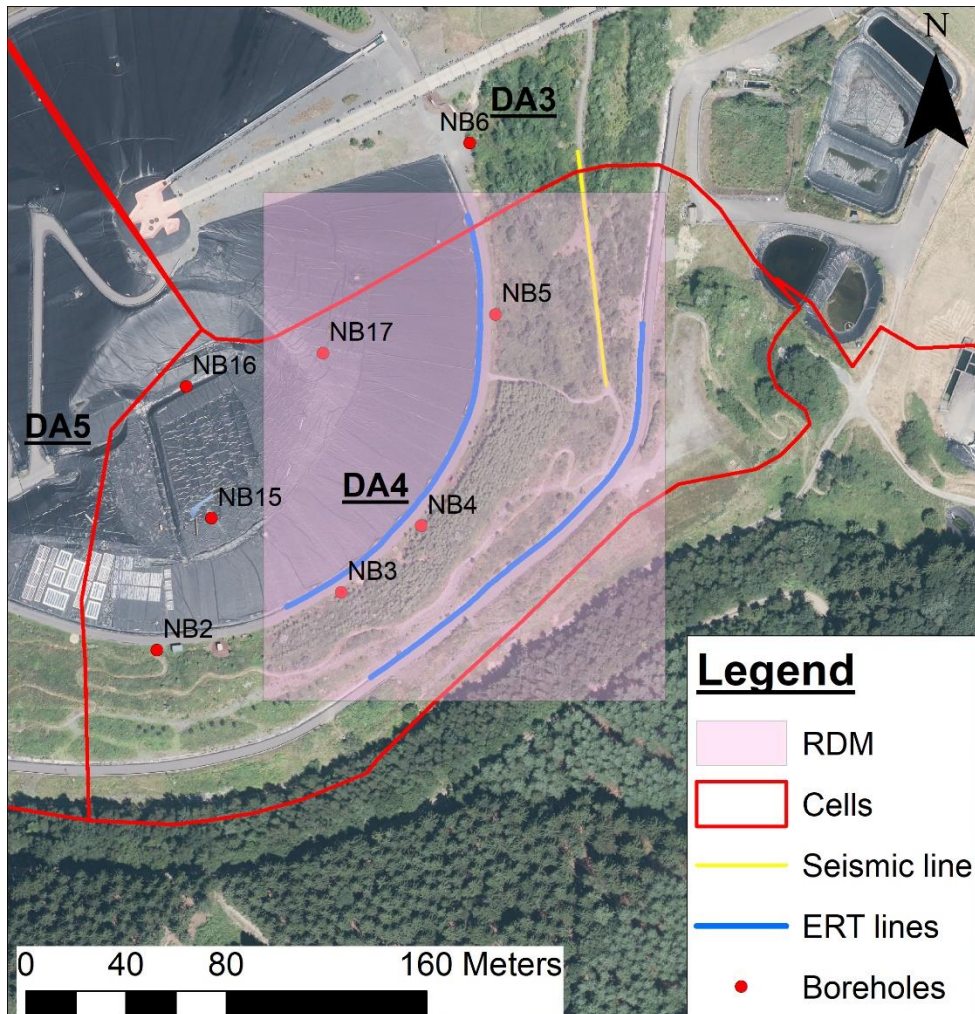


*Figure 13: Extent of the detailed RDM.*

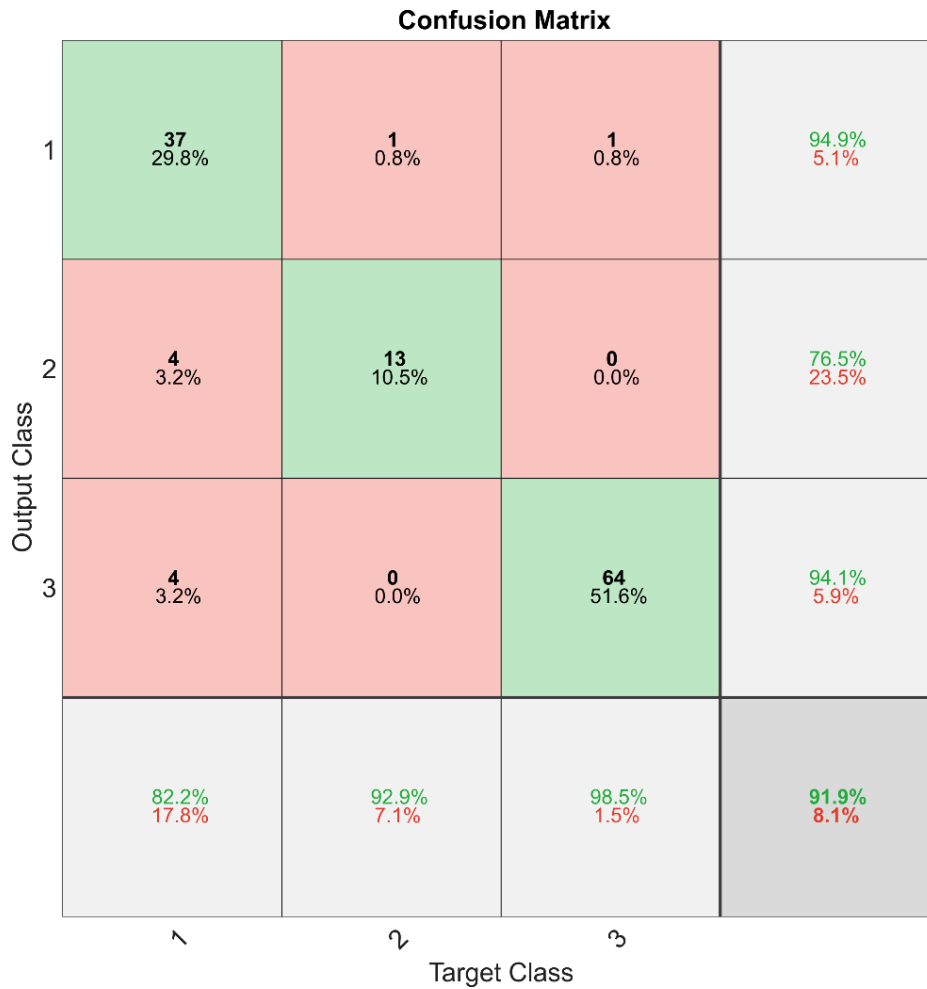
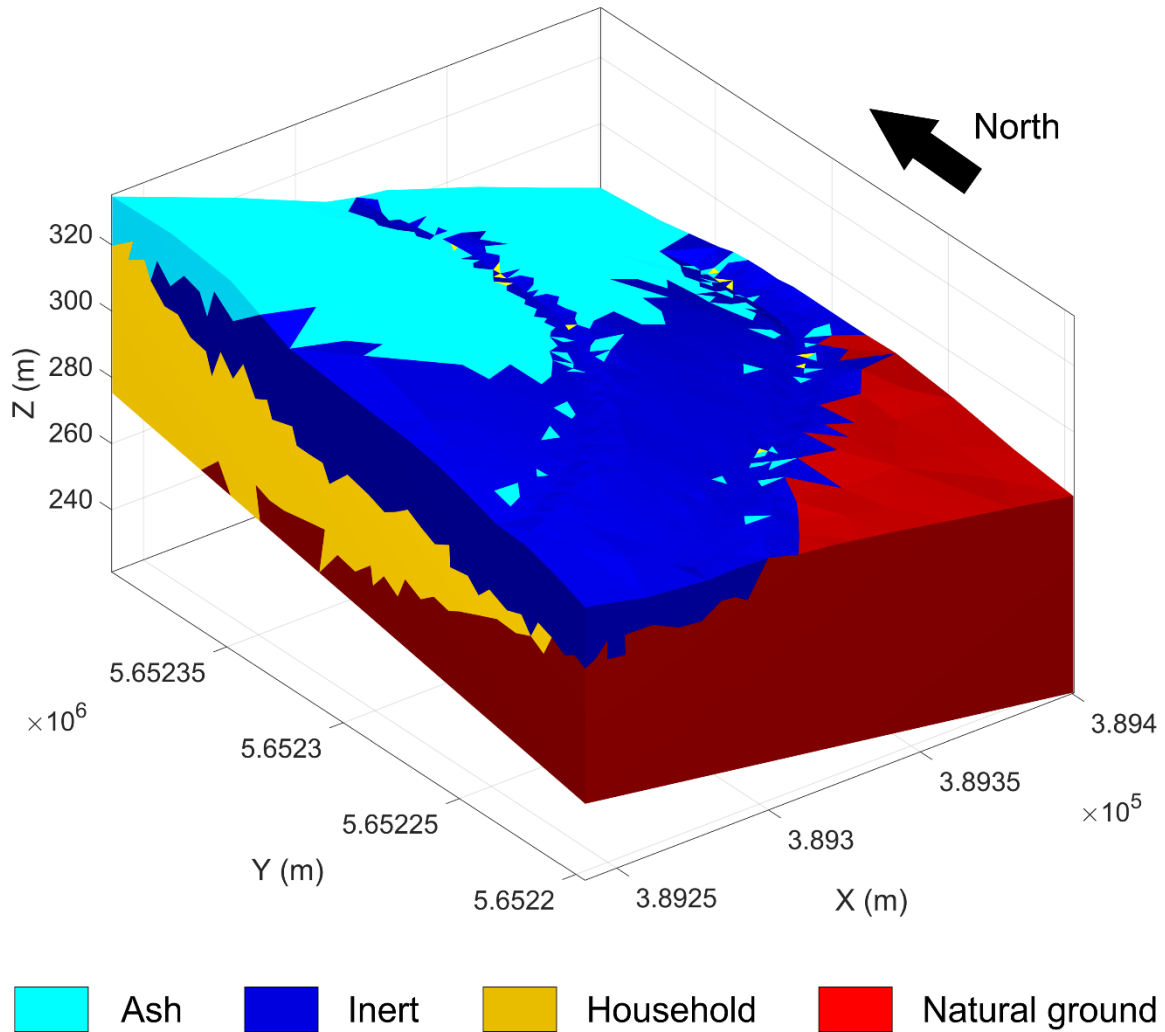


Figure 38: Confusion matrix measuring the performance of the machine learning classification.

Table 1: Estimation of the volumes of the defined material classes based on the classification performed by the neural network.

	<b>Estimated volume (m<sup>3</sup>)</b>
<b>Inert materials</b>	198,000
<b>Ash</b>	152,000
<b>Household waste</b>	453,000
<b>Natural ground</b>	1,350,000

### Resource distribution model



*Figure 39: Resource distribution model of the surveyed area obtained with after training a neural network for pattern recognition.*

## Conclusion

The geophysics acquisition in Leppe was challenging due to the topography and the infrastructure (e.g. presence of a geomembrane, thickness of deposits). For the ERT/IP survey, it was not trivial to plan a suitable array for the 3D acquisition and it was adapted to the zones where the drilling through the geomembrane could be more easily repaired. The HVSRR data was noisy due to the daily activities of the site (e.g. trucks passing nearby, machinery, recreational activities), but this was mitigated by increasing the recording time up to 20 minutes. For the MASW acquisition, we had to move the location of the profile in order to find a zone allowing a better coupling and a smooth surface. For these reasons, it was not possible to deploy all the methods in co-located areas.

The ERT/IP methods allowed to delineate the transition from inert waste to household/ash deposits, but the resolution/sensitivity was not sufficient to individually identify and locate these materials with certainty. In addition, because of the low resistivity observed, only limited depth of investigation could be achieved. Nevertheless, the IP method reveals the most promising for estimating waste types and volumes in zones with good coverage. The latter can only be improved by deploying more electrodes, which could be complicated due to the configuration of the site.

For the MASW method, we could derive a 2D section of the Shear-wave velocity, where it was possible to detect at least two heterogeneous layers. The velocities in these layers might correspond to the velocities of ash (on the top) and household waste (below). In addition, a possible third layer, the deepest one, characterized by higher velocities, was detected and might correspond to a transition with the natural soil.

The HVSRR results after the parametric analysis proved to be useful to map the bottom of the landfill. To this purpose we assumed a bi-layer model with a layer of ash on the top of a layer of household waste and we used the Shear-wave velocities derived from the MASW method to estimate the thickness of these deposits. The results obtained coincides almost perfectly with topography data before the landfilling activities on site started.

To derive the resource distribution model, the combination of geophysical, remote sensing, historical and sampling data allowed 1) to estimate the whole volume of the landfill and 2) to divide the surveyed zone into different material classes and to estimate their volume. The detailed RDM was achieved using a supervised machine learning algorithm that allowed to classify the geophysical parameters in three waste categories. Despite the limited amount of available data, the classification operated by the algorithm is in accordance with landfill structure and ground truth data from the boreholes and can be considered as a good estimation of the waste contained in the surveyed zone.

## References

Dahlin, T. and Zhou, B. (2006) Multiple-gradient array measurements for multichannel 2D resistivity imaging. *Near Surface Geophysics* 4(2), 113-123.

Günther, T., Rücker, C. and Spitzer, K. (2006) Three-dimensional modelling and inversion of DC resistivity data incorporating topography—II. Inversion. *Geophysical Journal International* 166(2), 506-517.

## Contact

Feel free to contact us.

### Coordination office:

---

<b>BELGIUM</b>	SPAQuE Boulevard M. Destenay 13 4000 Liège	c.neculau@spaque.be
----------------	--	---------------------

---

### Contact details of the project partners:

---

<b>BELGIUM</b>	Atrasol Cleantech Flanders / VITO OVAM Université de Liège	renaud.derijdt@atrasol.eu alain.ducheyne@vito.be ewille@ovam.be f.nguyen@ulg.ac.be
<b>FRANCE</b>	SAS Les Champs Jouault	champsjouault@gmail.com
<b>GERMANY</b>	BAV	pbv@bavmail.de
<b>THE UK</b>	NERC	jecha@bgs.ac.uk

---

